

Improving the optical properties of thin film plasmonic solar cells of InP absorber layer using nanowires

Abedin Nematpour¹, Mahmoud Nikoufard^{2}*

¹ Department of Nanoelectronics, Nanoscience and Nanotechnology Research Center, University of Kashan, Kashan, Iran

² Department of Electronics, Faculty of Electrical and Computer Engineering, University of Kashan, Kashan 87317-51167, Iran

Received 14 April 2020;

revised 25 June 2020;

accepted 09 July 2020;

available online 15 July 2020

Abstract

In this paper, a thin-film InP-based solar cell designed and simulated. The proposed InP solar cell has a periodic array of plasmonic back-reflector, which consists of a silver layer and two silver nanowires. The indium tin oxide (ITO) layer also utilized as an anti-reflection coating (ARC) layer on top. The design creates a light-trapping structure by using a plasmonic back-reflector and an anti-reflection coating layer on top, which increase the light absorption in the solar cell. The enhancement of light trapping was observed in the proposed configuration of the solar cell with an 1000 nm thick InP absorption layer, which improved the short-circuit current density and efficiency. The highest short-circuit current density and efficiency were determined 32.07 mA/cm² and 26.6%, respectively, for the nanowire radiuses of $R_1=50$ nm and $R_2=120$ nm. Therefore, this structure improves the ultimate efficiency of 38% compared with the InP-based solar cells counterparts.

Keywords: Efficiency; InP Material; Light Trapping; Nanowire; Plasmonic Solar Cell; Short-Circuit Current Density.

How to cite this article

Nematpour A., Nikoufard M. Improving the optical properties of thin film plasmonic solar cells of InP absorber layer using nanowires. *Int. J. Nano Dimens.*, 2020; 11 (3): 290-298.

INTRODUCTION

Thin film solar cells are a very important class of photovoltaic solar cells. They are recently the subject of intense researches, commercialization, and development efforts due to their high efficiency and low cost. The film thickness of thin film solar cells is in the range of few micrometers or less when high absorptive materials are used [1, 2]. The thickness of the solar cell is a very important parameter in the optimization procedure [3]. In all solar cells, there is a trade-off between absorption of light, which has a higher rate in the thicker device, and carrier collection, due to a shorter transport length in thinner solar cells [4]. Therefore, a physically thin but optically thick solar cell is very desirable. It can be achieved by

light trapping in the solar cell materials [5, 6]. Light trapping leads to more absorption and thus more generated electron and hole pairs [7]. This reduces the absorber layer thickness, which is beneficial in two cases of reducing the cost of the epitaxial growth of absorption layers and increasing the efficiency due to the shorter transportation length [7].

Light trapping in solar cells has played a significant role in improving the absorption performance of the device by multiple reflections within the absorption layer [4]. It is possible to achieve efficient light-trapping by the formation of a wavelength-scale texture on the substrate and then the deposition of the thin-film solar cell on top, which causes a large increase in photocurrent [8]. Different light trapping structures, including

* Corresponding Author Email: mnik@kashanu.ac.ir

randomly or periodically textured surfaces, photonic crystals and plasmonic structures (such as nanoparticles of metal) have been intensively studied in various kinds of solar cells [9, 10]. Metal nanoparticles like silver and gold interact strongly with infrared and visible photons due to the excitation of localized surface plasmons (LSPs) [4]. Silver and gold are the most broadly used materials, since their surface plasmon resonances situated in the visible spectral range. Silver (Ag) is usually considered to have a good optical property for plasmonic applications in photovoltaic efficiency enhancement and has a strong resonance and low absorption in the visible and near-infrared part of the solar spectrum [9].

Biswas *et al.* [11, 12] designed a photonic crystal back reflector for a-Si:H solar cells and compared their results with the classical $4n^2$ limit. The design considers a 2-D photonic crystal with tapered cones in a triangular lattice to improve the efficiency of the solar cell. They have reported the weighted absorption of 89% with nc-Si absorber layer thickness of 1 μm . Pillai *et al.* demonstrated an overall enhancement of photocurrent of 33% on silicon-on-insulator geometry with 1.25 μm thick absorption layer, respectively, by depositing silver nanoparticles on the surface of the solar cells. Ouyang *et al.* showed the short-circuit current density enhancement of 27% on thin film silicon solar cell employing self-assembled silver nanoparticles on the rear surface of the solar cell [4]. Ghosh *et al.* have been reported a short-circuit current of 24.59 mA/cm^2 and an open circuit voltage of 491 mV for InP/nano-Ag (6 nm)/CdS solar cell [13]. A short-circuit current density of 2 mA/cm^2 was determined without the deterioration of open-circuit voltage and fill factor by using Ag nanoparticles as a plasmonic back reflector [4]. A solar cell using InP nanowire array solar cells was reported with an efficiency of 13.8% and short-circuit current density of 24.6 mA/cm^2 [14]. When the roughened silver is used as a back reflector, the localized surface plasmons will be increased [15]. The size and shape of the metal particles affect the light scattering in plasmonic back reflector solar cells. Chen *et al.* demonstrated that the particles with a size of 200 nm show an enhancement in short-circuit current density (J_{sc}) in comparison to the smaller particles [16], which has been confirmed by other refs [8, 17]. Larger particles cause more scattering of light in the wider distribution angles with higher absorption.

InP material has a direct band gap of 1.34 eV [13, 19] equivalent wavelength of 925 nm, which is suitable for the solar spectrum. InP-based solar cells are also very desirable for space solar cells applications on account of their special tolerance to radiation [14, 20]. Sumaryada *et al.* were calculated an efficiency of 18.73% for a AlGaAs/InP/Ge multi-junction solar cell [19]. Vidur Raj *et al.* was fabricated the InP solar cell with an open-circuit voltage and an efficiency of 819 mV and 18.12%, respectively [21]. Also, Yin *et al.* have been demonstrated the InP heterojunction solar cell with an ultra-thin layer of 10 nm amorphous TiO_2 . The solar cell was shown a power conversion efficiency of 19.2% and a short-circuit current density of 30.5 mA/cm^2 [22]. In a new research, Kotlyar *et al.* have been shown an open-circuit voltage of 0.37 V, a short-circuit current density of 10.6 mA/cm^2 for the InP/p-Si Photovoltaic Heterostructure [23].

In this article, we present a new solar cell with an InP absorption layer consisting of the silver nanowires back-reflector and InP nanowires at the top. This structure is a unique design to increase light trapping in a solar cell. The incident radiation is effectively scattered by the nanowires, which enhance the optical absorption by increasing the light path through the absorption layer while keeping a short path for carriers. Hence, the short-circuit current density is increased overall wavelengths in the solar spectrum. In comparison to other InP solar cells, the maximum short-circuit current density of 32.07 mA/cm^2 was obtained that is a good result for a thin-film solar cell in comparison with a short-circuit current density of 10.6 mA/cm^2 [23], a short-circuit current density of 24.6 mA/cm^2 [14] and a short-circuit current density of 30.5 mA/cm^2 [22]. In addition, the simulations show an ultimate efficiency of 26.6% that is greater than the obtained efficiencies of 19.2% [22] and 18.12% [21].

This paper organized as follows: "Materials and methods" section explains about the proposed structure and methodology. "Results and discussions" presented and discussed in next section. The effect of nanowires radius and absorption layer thickness on the absorption, short-circuit current density, and open-circuit voltage investigated in this section. Finally, "conclusions" section summarizes the paper results and presents the concluding remarks.

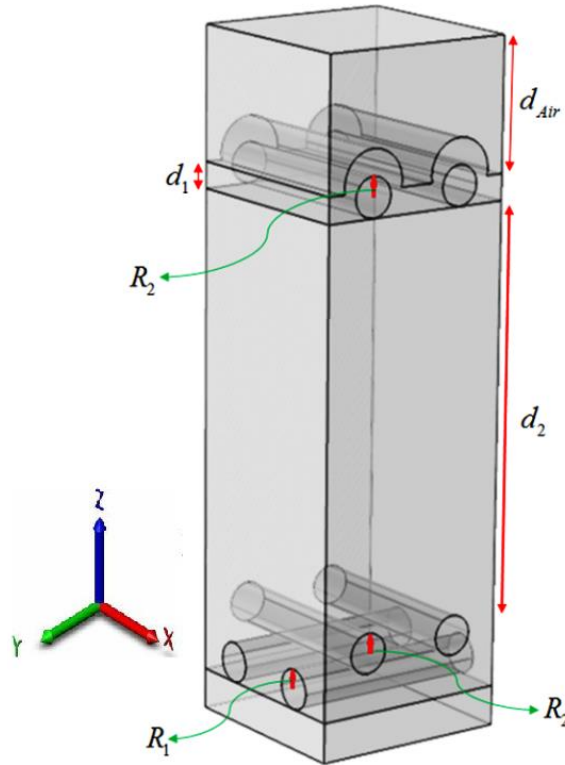


Fig. 1. Schematics of the solar cell a periodically textured device.

MATERIALS AND METHODS

The proposed thin-film solar cell divided into a number of layers in the z-direction as shown in Fig. 1. The solar cell layers consisted of the InP absorption layer, thickness of d_2 , two perpendicular Ag nanowires with radiuses of R_1 and R_2 in the bottom of absorption layer, and the InP nanowires with a radius of R_2 on the top of absorption layer, Ag back-reflector layer, and an anti-reflection layer of ITO on top with a thickness of d_1 . Center-to-center distance between the nanowires is $5R_1$ and the solar cell structure is periodic in the x and y directions.

Using the condition $A=1-R-T$, where A , R , and T are the absorption, total reflection and total transmission, respectively, the absorption can be found at each wavelength [24-27]. To obtain a realistic solar cell performance, the AM 1.5G spectrum was utilized in the simulations, resulting in $A(\lambda)$ over the entire spectrum. The absorption at each incident wavelength, $A(\lambda)$, can be determined by monitoring the incident power, $P_{in}(\lambda)$, and output power, $P_{out}(\lambda)$, as [7]:

$$A(\lambda) = \frac{P_{in}(\lambda) - P_{out}(\lambda)}{P_{in}(\lambda)} \tag{1}$$

This helps to calculate the weighted absorption $\langle A_w \rangle$ [28-30]:

$$\langle A_w \rangle = \frac{\int_{\lambda_1}^{\lambda_2} A(\lambda)\psi(\lambda)d\lambda}{\int_{\lambda_1}^{\lambda_2} \psi(\lambda)d\lambda} \tag{2}$$

Where $\psi(\lambda)$ is the incidence solar flux per unit wavelength, $\lambda_1=400\text{nm}$, and $\lambda_2=920\text{ nm}$. The short-circuit current density (J_{sc}) can also be calculated using [31, 32]

$$J_{sc} = \frac{e}{hc} \int_{\lambda_1}^{\lambda_2} \lambda A(\lambda)\psi(\lambda)d\lambda \tag{3}$$

Where e , h and c are the electron charge density, the Planck constant, and the speed of light in vacuum, respectively. The short-circuit current density, J_{sc} , is proportional to the number of photons within the wavelength range of λ_1 to λ_2 . It is assumed that each absorbed photon generates an electron-hole pair and all photogenerated carriers reach to the electrodes in which contributes to the photocurrent [33, 34].

Two important parameters of a solar cell are open-circuit voltage and efficiency. The open circuit voltage is the maximum voltage of a solar cell that can provide to an external circuit [35]:

$$V_{oc} = \frac{kT}{q} \ln\left(\frac{J_{sc}}{J_0} + 1\right) \quad (4)$$

Where, J_0 is the reverse saturation current density. The efficiency is the ratio of the maximum output power to the input power:

$$\eta = \frac{V_{oc} J_{sc} FF}{P_{in}} \quad (5)$$

Where fill factor (FF) is explained as the ratio of the maximum output power at the maximum power point to the product of V_{oc} and J_{sc} [35].

Simulations were carried out based on a well-determinate finite element method (FEM) using the Wave Optics, Frequency Domain interface of Comsol Multiphysics software. In this method Helmholtz equation, discretized in the solar cell structure. The three-dimensional (3D) solar cell structure was discretized using free triangular mesh. Materials selected with the wavelength-dependent refractive index to cover the wavelength range of visible and near infrared.

RESULTS AND DISCUSSIONS

A solar cell with plasmonic back-reflector and an anti-reflection coating is one of the best light trapping structures to increase solar cell efficiency. The geometry, shown in Fig. 1, simulated with a periodic boundary condition. We used the electromagnetic simulation to determine the absorption of light in the InP absorption layer on the conformal periodically textured back reflector. Nanowires back reflector and nanowires on the top of device have been shown large absorption

enhancement by light trapping effect.

The absorption of incident light ($A(\lambda)$) as a function of wavelength is shown in Fig. 2 in the visible and infrared spectrum range of $\lambda=400$ nm to 920 nm. The cavity between the Ag back-reflector nanowires and the top ITO layer caused the dropping of the absorption in some wavelengths dramatically, in which it depends on the radius of the nanowires. Meanwhile, the absorption of light shows highest values in the spectrum range of 400 nm-600 nm for nanowires radius of 70 nm, while it is the highest in the spectrum range of 750 nm-920 nm for nanowires radius of 50 nm. The highest absorption shows the good light trapping in the solar cell. Light trapping is the first characteristic to have high efficiency in the solar cell. In addition, the wavelength-dependence of absorption and light trapping showed in Fig. 2.

The weighted absorption was determined for a cell with a $d_1=65$ nm thick ITO layer, the InP absorption layer of $d_2=1000$ nm, and the scanned nanowires radiuses ($R=R_1=R_2$) from 30 nm to 120 nm, shown in Fig. 3 (a, b, c). The thickness of the ITO anti-reflection coating must satisfy the relation $d_1 = \lambda/4n$, where λ and n are the incident wavelength and refractive index of the anti-reflection coating layer, respectively, with considering the peak emission of solar radiation at $\lambda=500$ nm. We also calculated the short-circuit current density (J_{sc}) and open-circuit voltage (V_{oc}), shown in Figs. 3(b) and 3(c), respectively. The short-circuit current density and open-circuit voltage increase by increasing the radius of the nanowires (R). The maximum values for J_{sc} and V_{oc} can be observed around $R=110$ nm

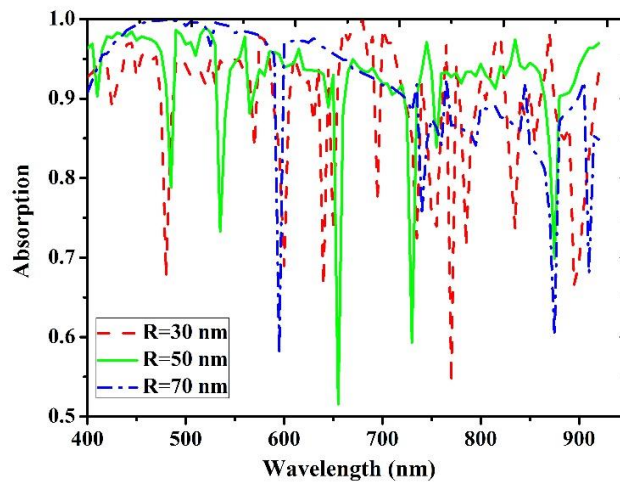


Fig. 2. Absorption as a function of wavelength for the solar cells with different radius of $R=30$ nm, 50 nm, 70 nm ($R=R_1=R_2$, $d_1=65$ nm and $d_2=1000$ nm).

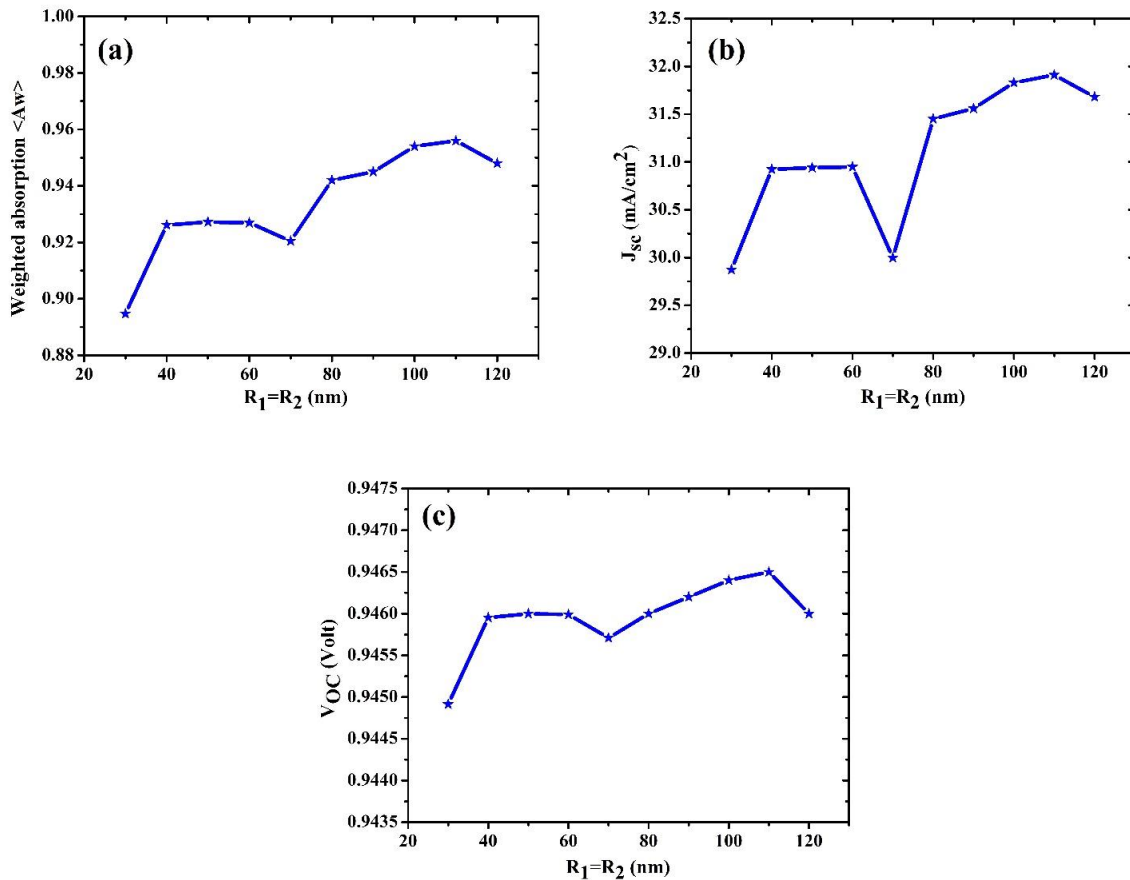


Fig. 3. (a) The weighted absorption $\langle A_w \rangle$ (b) the short-circuit current density (J_{sc}) (c) open-circuit voltage (V_{oc}) as a function of nanowires radius of R for $d_1=65$ nm and $d_2=1000$ nm.

whereas there are no significant changes in J_{sc} and V_{oc} within the range of $R=40$ nm to $R=60$ nm. A little drop in J_{sc} and V_{oc} can be observed for $R=70$ nm due to the less scattering of the optical field within the absorption layer.

In order to obtain the optimized structure, it found the radii of the nanowires with making the best light trapping in the solar cell because there is a modified between the radii of the nanowires and light trapping. The weighted absorption, short-circuit current density, and open-circuit voltage were determined for a 1000 nm thick absorption layer, $R_1=50$ nm, and different radii of R_2 , shown in Fig. 4 (a, b, c). The weighted absorption and short-circuit current density increase with increasing R_2 , reaching to the maximum value at $R_2=120$ nm ($\langle A_w \rangle = 0.96$ and $J_{sc} = 32.07$ mA/cm²). Similarly, the weighted absorption, short-circuit current density and open-circuit voltage were obtained for $R_2=50$ nm and different radii of R_1 ,

shown in Fig. 5 (a, b, c). The weighted absorption and short-circuit current density shows oscillations with increasing R_1 , where the maximum short-circuit current density is at $R_1=60$ nm. The light trapping increases because of plasmonic effect and the special structure of the solar cell. By considering Fig. 4 and Fig.5, the radii of the nanowires in the structure play an important role in light trapping in the solar cell.

Fig. 6 also illustrates the efficiency of the proposed solar cell for different nanowires radii. The results show that the efficiency is approximately constant since the radius of $R=R_1=R_2$ varies from 40 nm to 60 nm. By changing R_2 from 30 nm to 120 nm, there is an increase in efficiency and the maximum efficiency is equal to 0.266 (26.6 %) at $R_2=120$ nm for $R_1=50$ nm. Moreover, the efficiency increases by incrementing R_1 from 30 nm to 120 nm by keeping $R_2=50$ nm, in which the maximum efficiency is obtained equal to 0.259

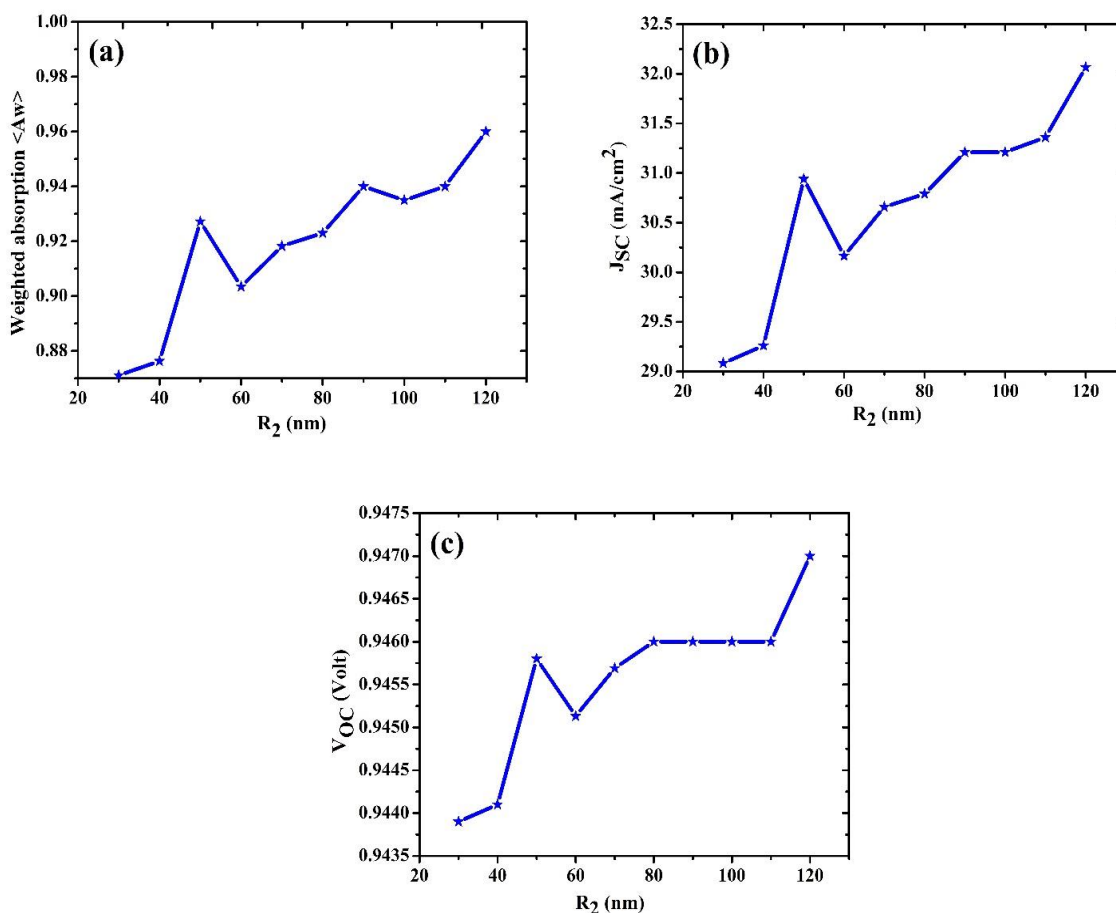


Fig. 4. (a) The weighted absorption $\langle A_w \rangle$ (b) short-circuit current density (J_{sc}) (c) open-circuit voltage (V_{oc}) as a function of R_2 ($R_1=50$ nm, $d_1=65$ nm, and $d_2=1000$ nm).

(25.9 %) at $R_1=60$ nm. In addition, the maximum efficiency was determined equal to 0.265 (26.5 %) at $R=110$ nm. Efficiency enhancement is due to the plasmonic nature of solar cell structure. If the shape and size of metal nanowire is suitably chosen then it will lead to the formation of surface plasmon polaritons, which propagate parallel to the metal surface and as a result increasing the light intensity absorption in the InP absorption layer.

The lateral propagation of the electrical field in the InP region can be observed by plotting the Poynting vector, shown in Fig 7, where light trapping can be seen in the solar cell structure. The Poynting vector is stochastically scattered through all angles within the absorption layer especially in the bottom, thereby increasing the path length of photons through the absorption layer.

CONCLUSIONS

In summary, in this paper we have presented a new nano-structure solar cell with a periodic array of plasmonic nanowire back-reflector, InP absorption layer and a layer of ITO as anti-reflection coating on top. The plasmonic back-reflector consists of a silver layer and two silver nanowires. This design helps to have a good light trapping in the solar cell structure. The 3D solar cell structure was simulated by the Wave Optics of Comsol Multiphysics to calculate the absorption, open-circuit voltage, short-circuit current density, and efficiency. The simulation results show the enhanced light trapping in the InP absorption layer with a maximum efficiency of 26.6 % for the nanowires radiuses of $R_1=120$ nm and $R_2=50$ nm. Therefore, the proposed plasmonic-based solar cell can increase the optical absorption in

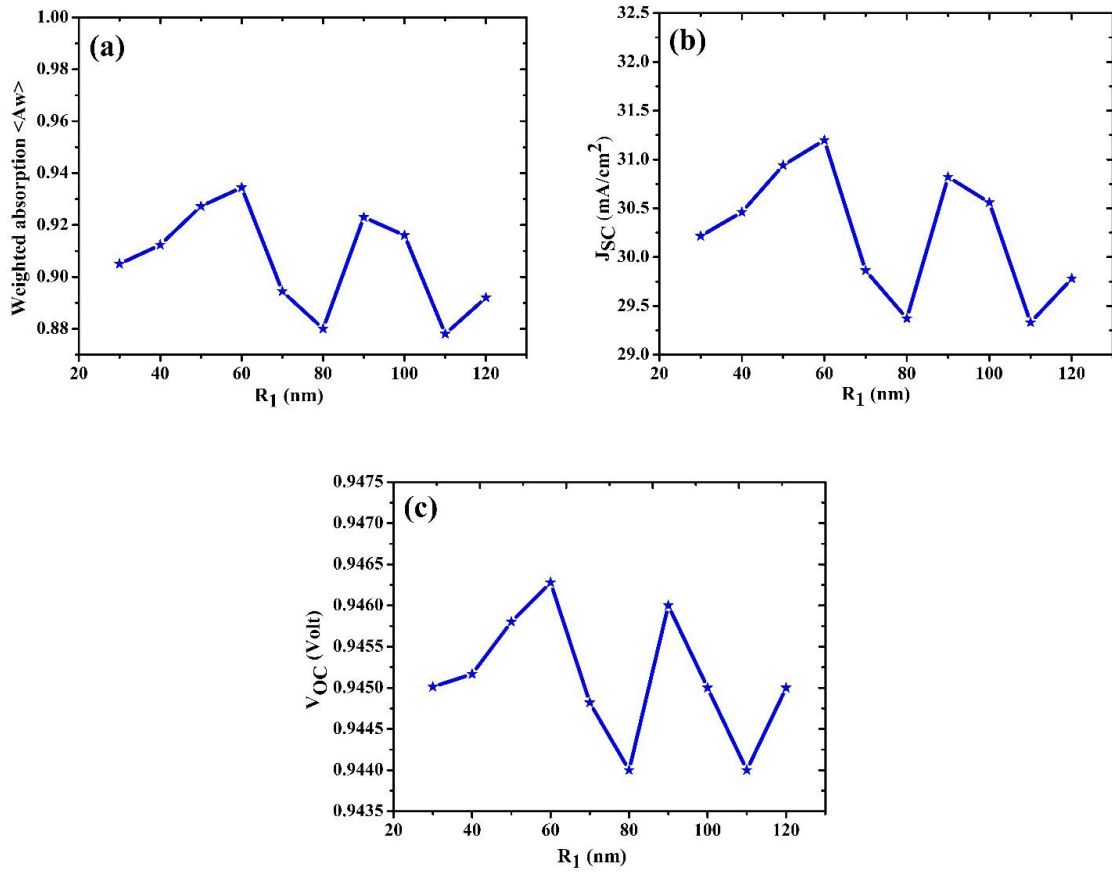


Fig. 5. (a) The weighted absorption $\langle A_w \rangle$ (b) the short-circuit current density (J_{sc}) (c) open-circuit voltage (V_{oc}) as a function of R_1 ($R_2=50$ nm, $d_1=65$ nm, and $d_2=1000$ nm).

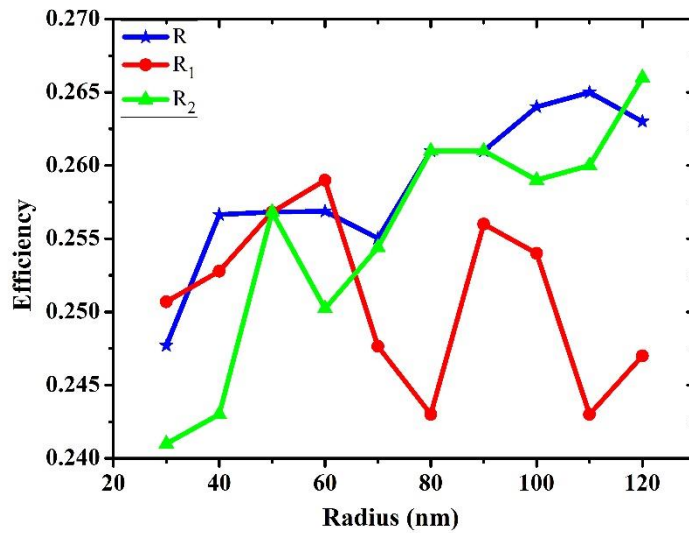


Fig. 6. Efficiency of solar cell versus the radius of the nanowires ($d_1=65$ nm and $d_2=1000$ nm).

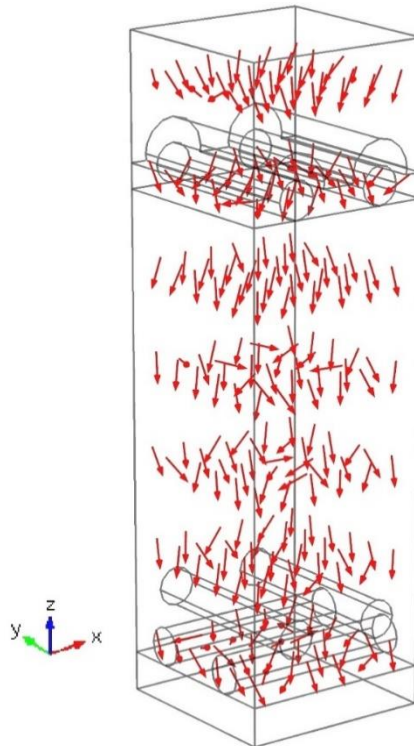


Fig. 7. The Poynting vector direction in the structure of InP-based solar cell.

the solar cell structure, allowing a considerable reduction in the absorption layer thickness. The main advantage of the proposed solar cell is an enhancement efficiency of 38% in comparison with other InP solar cells.

CONFLICT OF INTEREST

The authors declare that there is no conflict of interest.

REFERENCES

- [1] Cai T., Han S. E., (2015), Effect of symmetry in periodic nanostructures on light trapping in thin film solar cells. *JOSA B*. 32: 2264-2270.
- [2] Girigoswami K., Akhtar N., (2019), Nanobiosensors and fluorescence based biosensors: An overview. *Int. J. Nano Dimens*. 10: 1-17.
- [3] Anderson T. H., Benjamin J. C., Peter B. M., Akhlesh L., (2020), Coupled optoelectronic simulation and optimization of thin-film photovoltaic solar cells. *J. Comput. Phys*. 407: 109242.
- [4] Miao X., Tongay S., Petterson M. K., Berke K., Rinzler A. G., Appleton B. R., Hebard A. F., (2012), High efficiency graphene solar cells by chemical doping. *Nano Lett*. 12: 2745-2750.
- [5] Wang F., Yuhong Z., Meifang Y., Lin F., Lili Y., Yingrui S., Jinghai Y., Xiaodan Z., (2019), Toward ultra-thin and omnidirectional perovskite solar cells: Concurrent improvement in conversion efficiency by employing light-trapping and recrystallizing treatment. *Nano Energy*. 60: 198-204.
- [6] Shi L., Zhou Z., Tang B., (2014), Optimization of Si solar cells with full band optical absorption increased in all polarizations using plasmonic backcontact grating. *Opt. Int. J. Light and Electron Optic*. 125: 789-794.
- [7] Sethi V., Pandey M., Shukla M. P., (2011), Use of nanotechnology in solar PV cell. *Int. J. Chem. Eng. Appl*. 2: 77-83.
- [8] Catchpole K., Polman A., (2008), Plasmonic solar cells. *Optics Express*. 16: 21793-21800.
- [9] Haidari G., Hajimahmoodzadeh M., Fallah H. R., Varnamkhasti M. G., (2015), Effective medium analysis of thermally evaporated Ag nanoparticle films for plasmonic enhancement in organic solar cell. *Superlatt. Microstruc*. 85: 294-304.
- [10] Sagadevan S., Pandurangan K., (2015), Investigations on structural and electrical properties of Cadmium Zinc Sulfide thin films. *Int. J. Nano Dimens*. 6: 433-438.
- [11] Biswas R., Bhattacharya J., Lewis B., Chakravarty N., Dalal V., (2010), Enhanced nanocrystalline silicon solar cell with a photonic crystal back-reflector. *Solar Energy Mater. Solar Cells*. 94: 2337-2342.
- [12] Biswas R., Zhou D., (2008), Improved photon absorption in a-Si : H solar cells using photonic crystal architectures, (Cambridge Univ Press), 1066: A14-04.
- [13] Ghosh D., Ghosh B., Hussain S., Chakraborty B., Sehgal G., Bhar R., Pal A., (2014), Improvement on the performance of InP/CdS solar cells with the inclusion of plasmonic layer

- of Silver nanoparticles. *Plasmonics*. 9: 1271-1281.
- [14] Wallentin J., Anttu N., Asoli D., Huffman M., Åberg I., Magnusson M. H., Siefer G., Fuss-Kailuweit P., Dimroth F., Witzigmann B., (2013), InP nanowire array solar cells achieving 13.8% efficiency by exceeding the ray optics limit. *Science*. 339: 1057-1060.
- [15] Pattnaik S., Chakravarty N., Biswas R., Dalal V., Slafer D., (2014), Nano-photonic and nano-plasmonic enhancements in thin film silicon solar cells. *Solar Energy Mater. Solar Cells*. 129: 115-123.
- [16] Chen X., Jia B., Saha J. K., Cai B., Stokes N., Qiao Q., Wang Y., Shi Z., Gu M., (2012), Broadband enhancement in thin-film amorphous silicon solar cells enabled by nucleated silver nanoparticles. *Nano Lett.* 12: 2187-2192.
- [17] Chou C.-H., Chen F.-C., (2014), Plasmonic nanostructures for light trapping in organic photovoltaic devices. *Nanoscale*. 6: 8444-8458.
- [18] Song Y., Peng B. D., Xu Q., Cao N., Song G. Z., Yue Z. Q., Li B. K., Wang H. X., (2018), A method for demonstration of the feasibility of InP as an All-optical imaging sensor. *Opt. Sens.* ISBN: 978-1-943580-43-9.
- [19] Sumaryada T., Rohaeni S., Damayanti N. E., Syafutra H., Hardhienata H., (2019), Simulating the performance of AlO₃/GaO₃/InP/Ge multijunction solar cells under variation of spectral irradiance and temperature. *Modell. Simul. Eng.* 2019: Article ID 5090981.
- [20] Nematpour A., Nikoufard M., (2018), Plasmonic thin film InP/graphene-based Schottky-junction solar cell using nanorods. *J. Adv. Res.* 10: 15-20.
- [21] Raj V., Dos Santos T. S., Rougieux F., Vora K., Lysevych M., Fu L., Mokkapati S., Tan H. H., Jagadish C., (2018), Indium phosphide based solar cell using ultra-thin ZnO as an electron selective layer. *J. Phys. D: Appl. Phys.* 51: 395301-395306.
- [22] Yin X., Battaglia C., Lin Y., Chen K., Hettick M., Zheng M., Chen C.-Y., Kiriya D., Javey A., (2014), 19.2% efficient InP heterojunction solar cell with electron-selective TiO₂ contact. *ACS Photon.* 1: 1245-1250.
- [23] Kotlyar K. P., Vershinin A. V., Reznik R. R., Pavlov S. I., Kudryashov D. A., Zelentsov K. S., Mozharov A. M., (2019), Photovoltaic properties of InP NWs/p-Si heterostructure. *J. Phys.: Conf. Series*. 1410: 012060-012067.
- [24] Wang Y., Zhang X., Guo M., Sun X., Yu Y., Xi J., (2015), Needle profile grating structure for absorption enhancement in GaAs thin film solar cells. *Opt. Laser Technol.* 74: 43-47.
- [25] Lagos N., Sigalas M., Niarchos D., (2011), The optical absorption of nanowire arrays. *Photon. Nanostruc. Fundament. Applic.* 9: 163-167.
- [26] Tabrizi A. A., Pahlavan A., (2020), Efficiency improvement of a silicon-based thin-film solar cell using plasmonic silver nanoparticles and an antireflective layer. *Opt. Commun.* 454: 124437-124443.
- [27] Choi M., Kang G., Shin D., Barange N., Lee C.-W., Ko D.-H., Kim K., (2016), Lithography-free broadband ultrathin-film absorbers with gap-plasmon resonance for organic photovoltaics. *ACS Appl. Mater. Interf.* 8: 12997-13008.
- [28] Zhong Y.-K., Fu S.-M., Ju N. P., Lin A., (2015), Toward ultimate nanophotonic light trapping using pattern-designed quasi-guided mode excitations. *JOSA B*. 32: 1252-1258.
- [29] Wang Y., Zhang X., Sun X., Qi Y., Wang Z., Wang H., (2016), Enhanced optical properties in inclined GaAs nanowire arrays for high-efficiency solar cells. *Opt. Laser Technol.* 85: 85-90.
- [30] Yin Y., Yu Z., Liu Y., Ye H., Zhang W., Cui Q., Yu X., Wang P., Zhang Y., (2014), Design of plasmonic solar cells combining dual interface nanostructure for broadband absorption enhancement. *Opt. Commun.* 333: 213-218.
- [31] Biswas R., Xu C., (2011), Nano-crystalline silicon solar cell architecture with absorption at the classical 4n 2 limit. *Opt. Express*. 19: A664-A672.
- [32] Nematpour A., Nikoufard M., Mehragha R., (2018), Design and optimization of the plasmonic graphene/InP thin-film solar-cell structure. *Laser Phys.* 28: 066202-066208.
- [33] Ferry V. E., Sweatlock L. A., Pacifici D., Atwater H. A., (2008), Plasmonic nanostructure design for efficient light coupling into solar cells. *Nano Lett.* 8: 4391-4397.
- [34] Shi M., (2019), Effect of metallic grid on Solar cell reflectance spectrum simulation and optimization of antireflection film. *Photon. Energy*. ISBN: 978-1-943580-72-9.
- [35] Zerfaoui H., Djalel D., Burak K., (2019), The simulated effects of different light intensities on the SiC-based solar cells. *Silicon*. 4: 1917-1923.